# Supporting Information

# A hybrid of borotungstate-coated metal-organic framework with supercapacitance, photocatalytic dye degradation and $H_2O_2$ sensing properties

Liang Yu[a], Kang Ning[a], Wang Chunmei[a], Yu Kai[ab]*, Lv Jinghua[a], Wang Chunxiao[a], Zhou Baibin[ab]*

*Corresponding authors.

E-mail addresses: hlyukai188@163.com(K. Yu), zhou_bai_bin@163.com(B. Zhou)

## Table of Contents

# 1. Experimental section

### 1.1 Material characterization methods

Fourier transform infrared (FTIR) spectra of compound was carried out on a Nicolet-360 spectrophotometer in the range of 400-4000 $cm^{-1}$ using KBr particles. Use JEOL JSM-6700 M scanning electron microscope (SEM) produced by Hitachi to analyze the morphology and content. The transmission electron microscopy (TEM) images were performed on aultrahigh resolution scanning electron microscope (JEOL2010, Japan). Thermogravimetric analysis (TGA) is a PerkinElmer Diamond 6300 differential thermal analyzer produced in the United States, with α-$Al_2O_3$ as the reference material, using a platinum crucible, the heating rate is 10 ℃ $min^{-1}$, and the heating is 25℃ to 800℃, $N_2$ protects the atmosphere of the system. X-ray photoelectron spectroscopy (XPS) test equipment comes from Shimadzu Corporation, Japan, model is Axis Ultra DLD, after analyzing the element valence state and distribution of the sample. The specific surface area (BET) test instrument comes from the United States Kangta company, the model is Nova 2000E specific surface area analyzer. Powder X-ray diffraction (XRD, BRUKER D8) using Cu Kα radiation (λ= 0.154 nm) was employed to identify the crystalline phase of the material and the range of 2θ from 10-60°. The UV-2700 UV analyzer from Shimadzu Instruments was used for testing in the 200-800 nm wavelength range.

### 1.2 Synthesis of $K_5BW_{12}O_{40}•15H_2O$

Synthesis is performed according to reference.[1] With typical methods: Weigh 40 g $Na_2WO_4·2H_2O$ and 3 g $H_3BO_3$, dissolve in 60 mL distilled water, adjust the pH to 6 with 6 M HCl. Boil under magnetic stirring for 2 h, filter to remove impurities, after which the filtrate is adjusted to pH 2 with 6 M HCl. Add 80 g KCl, at which point a precipitate is formed in the solution, filter, wash with ether. The precipitate was filtered, washed with ether and dried to give 23.2 g of crude product.

### 1.3 Synthesis of $Ag_5[BW_{12}O_{40}]$

According to reference,[1] a typical method: $AgNO_3$ (0.2400 g, 1.142 mmol) and $K_5[BW_{12}O_{40}]·15H_2O$ (0.2800 g, 0.0918 mmol) were dissolved sequentially in 10 mL of distilled water and the solution was adjusted to pH=4 with 1 M KOH. The solvent was evaporated to dryness and then dried in an oven at 60°C for 24 h to obtain a grey powdered sample of $Ag_5[BW_{12}O_{40}]$.

### 1.4 Synthesis of Ag-BTC

According to reference,[2] a typical method: $AgNO_3$ (0.2400 g, 1.412 mmol) and $H_3BTC$ (0.1400 g, 0.6667 mmol) were mixed in an agate mortar and ground for 20 min, after which they were washed with ethanol and distilled water and dried in an oven at 60°C for 24 h to obtain a grey powdered sample of Ag-BTC.

### 1.5 Electrode preparation

**Preparation of Nickel foam electrode**：The active substance was prepared by mixing acetylene black with {$Ag_5BW_{12}O_{40}$}@Ag-BTC-n in the weight ratio of 1:4, sonicated for 50 min, and oven dried at 50°C. Dissolve 5mg active substance in 150 μL ethanol solution (ethanol: water = 1:3), ultrasonic dispersion for 40min to make a slurry, evenly pasted on nickel foam (1×3$cm^2$) (one side), dried in a vacuum oven at 50℃ for 4h to remove the solvent. Then it was defined as {$Ag_5BW_{12}O_{40}$}@Ag-BTC-n-NF, $Ag_5[BW_{12}O_{40}]$-NF and Ag-BTC-NF were also prepared by this method.

**Preparation of symmetric supercapacitors:** Nickel foam coated with active substance was prepared and made available under pressure conditions of 2 MPa. The difference in mass before and after the nickel foam was attributed to the loading of the active substance. The mass loading of the active substance on each electrode was about 3 mg, and the current density (A $g^{-1}$) and specific capacitance (F $g^{-1}$) were calculated from the total mass of the active substance.

**Preparation of glass-carbon electrodes**：{$Ag_5BW_{12}O_{40}$}@Ag-BTC-2 was mixed with acetylene black as

raw material and ground into a slurry in a 3:1 ethanol solution. The dispersed slurry (5μL) was dropped on the glassy carbon electrode. A uniform film was formed after 2 hours at room temperature. The Nafion solution (5μL) is then dropped onto the electrode surface as a protective film. As a protective film drops are placed on the electrode surface and dried for 1 hour.

**1.6 Computational formula**

The specific capacitance of the three electrodes system is calculated as follow[3]:

$C_s = I \times \Delta t / (m \times \Delta V)$ Equation(S1)

where $I$(A $g^{-1}$) is the discharge current and $\Delta t$ (s)is the discharge time, $\Delta V$(V) is the voltage window, and $m$(g) is the load of the active material in the electrode.

The formula for calculating the specific capacitance of two electrodes[4]:

$C = 2I \times \Delta t / (m \times \Delta V)$ Equation(S2)

where $I$ is the current density (A $g^{-1}$), $\Delta t$ designates the discharge time(s), $m$ signifies mass of both the electrodes (g) and $\Delta V$ represents voltage window (V), respectively. The energy density ($E$, Wh $kg^{-1}$) and power density ($P$, W $kg^{-1}$) calculation formulas are as follows:

$E = C\Delta V^2/7.2$ Equation(S3)

$P = E \times 3600/\Delta t$ Equation(S4)

Catalytic efficiency calculation formula:

CAT = 100% × [Ip{compound}$H_2O_2$ − Ip{compound}] / Ip {compound} Equation(S5)

## 2. Results and Discussion

**2.1 XRD、BET and TG**

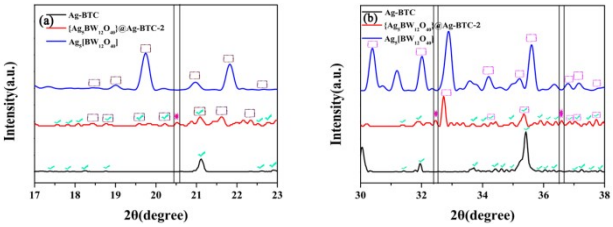


**Figure S1.** Local XRD images of three compounds

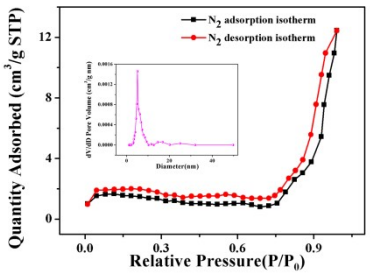


**Figure S2.** $N_2$ absorption-desorption isotherm of {$Ag_5BW_{12}O_{40}$}@Ag-BTC-2. (Insets are the aperture distribution map)

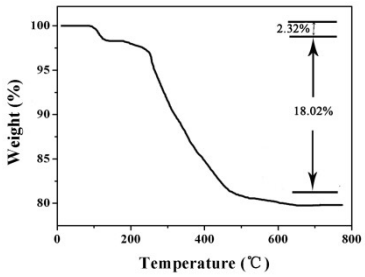


**Figure S3.** The TG curve of $\{Ag_5BW_{12}O_{40}\}$@Ag-BTC-2

## 2.2 Electrochemical properties

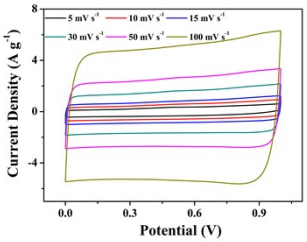


**Figure S4.** CV curves of the SC with the different scan rates

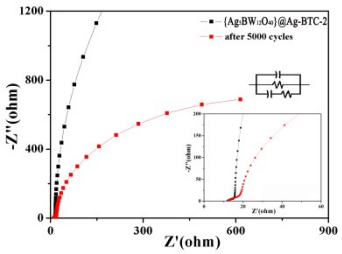


**Figure S5.** EIS test chart of the SC

## 2.3 Photocatalytic of $\{Ag_5BW_{12}O_{40}\}$@Ag-BTC-2

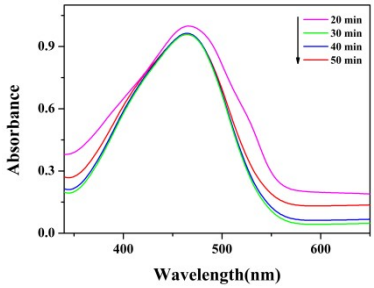


**Figure S6.** UV absorption spectra of MO aqueous solutions at different times in a dark room.

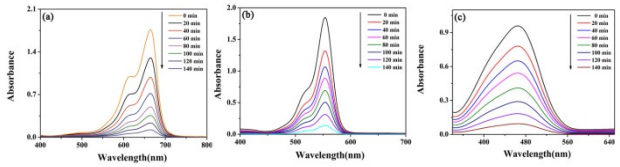


**Figure S7.** UV absorption spectra for (a)MB, (b)RhB and (c)MO aqueous solution during photodegradation with $\{Ag_5BW_{12}O_{40}\}$@Ag-BTC-2.

### 2.4 Electrochemical sensing of $\{Ag_5BW_{12}O_{40}\}$@Ag-BTC-2

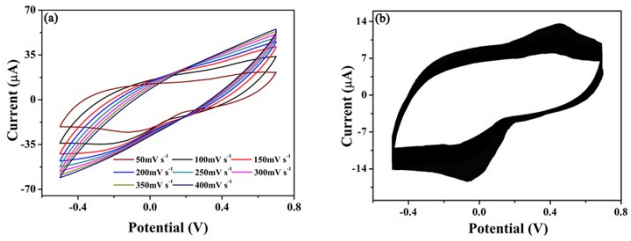


**Figure S8.** (a) CV in 0.1 M PBS buffer; (b) The CV curve of 1000 cycles at 50 mV $s^{-1}$ in 0.1 M PBS solution

## Table S1. Comparison of the properties of the Keggin POMs-based materials with several published supercapacitors

| | materials | specific capacitance | cycling stability | current collector | Ref. |
|---|---|---|---|---|---|
| 1 | Zn-BTC@$Ag_5[BW_{12}O_{40}]$ | 161.7 F $g^{-1}$ (1 A $g^{-1}$) | 92.8% (5000 cycles) | nickel foam | 1 |
| 2 | $Ag_5[BW_{12}O_{40}]$ | 97.7 F $g^{-1}$ (1 A $g^{-1}$) | 84.4% (5000 cycles) | nickel foam | 1 |
| 3 | $[Cu^{I}H_2(C_{12}H_{12}N_6)(PMo_{12}O_{40})]\cdot[(C_6H_{15}N)(H_2O)_2]$ | 249.0 F $g^{-1}$ (3 A $g^{-1}$) | 93.5% (1000 cycles) | glassy carbon | 5 |
| 4 | PAni-$PMo_{12}$ | 172.38 F $g^{-1}$ (1 A $g^{-1}$) | | stainlss steel | 5 |
| 5 | $[Mn_2(BTC)_4/3(H_2O)_6]_6[K_8(SiW_{10}Mn_2Cl_4O_{36})]$ | 211.0 F $g^{-1}$ (1 A $g^{-1}$) | 96.0% (5000 cycles) | nickel foam | 6 |
| 6 | $PW_{12}$@MIL-101 | 158 mF·$cm^{-2}$ (0.5 mA·$cm^{-2}$) | | nickel foam | 7 |
| 7 | $[BMIM]_4SiW_{12}O_{40}$ | 172 F $g^{-1}$ | 89% (1100 cycles) | glassy carbon | 8 |
| 8 | $[Ag_{10}(C_2H_2N_3)_8][HVW_{12}O_{40}]$ | 93.5 F $g^{-1}$ (1.5 A $g^{-1}$) | 59.2% (750 cycles) | glassy carbon | 9 |
| 9 | PAni/$H_3PMo_{12}O_{40}$ | 120F $g^{-1}$ | 70% (1000 cycles) | Rigid graphite plate | 10 |

| | | | | | |
|---|---|---|---|---|---|
| 10 | $[Ag_5(brtmb)_4][VW_{10}V_2O_{40}]$ | 206 F $g^{-1}$ (110 A $g^{-1}$) | 81.7% (1000 cycles) | glassy carbon | 11 |
| 11 | SWCNT/TBA/$PMo_{12}V_2O_{40}$ | 444 F $g^{-1}$ (10 mV $s^{-1}$) | 95% (6500 cycles) | glassy carbon | 12 |
| 12 | AC/$TEAPW_{12}$ | 82 F $g^{-1}$ (0.5 A $g^{-1}$) | 93% (10000 cycles) | alumin um foil | 13 |
| 13 | AC/$PMo_{12}O_{40}$ | 140 F $g^{-1}$ (1 A $g^{-1}$) | 91% (8000 cycles) | glassy carbon | 14 |
| 14 | AC/$PW_{12}O_{40}$ | 254 F $g^{-1}$ (10 mV $s^{-1}$) | 35% (30000 cycles) | Graphit e rods | 15 |
| 15 | $H_3PW^{VI}_{12}O_{40}\cdot(BPE)_{2.5}\cdot 3H_2O$ | 49.2 F $g^{-1}$ (2 A $g^{-1}$) | 80.4% (1000 cycles) | glassy carbon | 16 |
| 16 | $H_3PMo^{VI}_{12}O_{40}\cdot(BPE)_{2.5}\cdot 3H_2O$ | 137.5 F $g^{-1}$ (2 A $g^{-1}$) | 92.0% (1000 cycles) | glassy carbon | 16 |
| 17 | $[HPMo^{VI}_9Mo^{V}_3O_{40}]Cu^{I}_5$[4- atrz]$_6\cdot H_2O$ | 231.7 F $g^{-1}$ (1 A $g^{-1}$) | 88.2% (1000 cycles) | glassy carbon | 16 |
| 18 | $H_3PMo^{VI}_{12}O_{40}\cdot(BPE)_{2.5}\cdot 3H_2O$ | 137.5 F $g^{-1}$ (2 A $g^{-1}$) | 92.0% (1000 cycles) | glassy carbon | 16 |
| 19 | $L_{0.5}[Cu_2L_{3.5}(SiW_{12}O_{40})]$ | 159.2 F $g^{-1}$ (3 A $g^{-1}$) | | glassy carbon | 17 |
| 20 | $[HPW^{VI}_9W^{V}_3O_{40}]Cu^{I}_5$[4- atrz]$_6$ | 147.5 F $g^{-1}$ (1 A $g^{-1}$) | 95.3% (1000 cycles) | glassy carbon | 18 |
| 21 | $[H_2SiMo^{VI}_9Mo^{V}_3O_{40}]Cu^{I}_5$[4-atrz]$_6\cdot H_2O$ | 232.5 F $g^{-1}$ (1 A $g^{-1}$) | 98.8% (1000 cycles) | glassy carbon | 18 |
| 22 | mPPy@GO-$PMo_{12}$ | 115 mF $cm^{-2}$ (1 mV $s^{-1}$) | 80% (2000 cycles) | glassy carbon | 19 |
| 23 | rGO-$PMo_{12}$‖rGO-$PW_{12}$ | 110 F $cm^{-2}$ (2 mA $cm^{-2}$) | 95% (2000 cycles) | carbon cloth | 20 |
| 24 | $\{Ag_5BW_{12}O_{40}\}$@Ag-BTC-2 | 179.1 F $g^{-1}$ (1 A $g^{-1}$) | 97.4% (5000 cycles) | nickel foam | This work |

## References


1 L. Y. Wang, N. Kang, L. G. Gong, C. X. Wang, K. Yu, C. M. Wang and B. B. Zhou, *J Energy Storage*, 2022, **46**, 103873.

2 X. Y. Zhao, L. G. Gong, C. X. Wang, C. M. Wang, K. Yu and B. B. Zhou, *Chem. Eur. J.*, 2020, **26**, 4613–4619.

3 L. X. Zheng, C. D. Wang, Y. C. Dong, H. D. Bian, T. F. Hung, J. Lu and Y. Y. Li, *Appl. Surf. Sci.*, 2016, **362**, 399-405.

4 L. G. Gong, X. X. Qi, K. Yu, J. Q. Gao, B. B. Zhou and G. Y. Yang, J. Mater. Chem, A., 2020, **8**, 5709-5720.

5 D. F. Chai, J. J. Xin, B. N. Li, H. J. Pang, H. Y. Ma, K. Q. Li, B. X. Xiao, X. M. Wang and L. C. Tan, *Dalton Trans.*, 2019, **48**, 13026-13033.

6 Z. W. Zheng, X. Y. Zhao, L. G. Gong, C. X. Wang, C. M. Wang, K. Yu and B. B. Zhou, *J. Solid State Chem.*, 2020, **288**, 121409.

7 T. Y. Li, P. He, Y. N. Dong, W. C. Chen, T. Wang, J. Gong and W. L. Chen, *Eur. J. Inorg. Chem.*, 2021, **21**, 2063-2069.

8 M. Ammamz and J. Fransaer, *J. Electrochem Soc*., 2011, **158**, A14-A21.

9 Y. Hou, H. J. Pang, C. J. Gómez-García, H. Y. Ma, X. M. Wang and L. C. Tan, *Inorg. Chem.*, 2019, **58**, 16028-16039.

10 A. K. C. Gallegos, M. L. Cantú, N. C. Pastor and P. G. Romero, *Adv. Funct. Mater.*, 2005, **15**, 1125-1133.

11 G. N. Wang, T. T. Chen, X. M. Wang, H. Y. Ma and H. J. Pang, *Eur. J. Inorg. Chem.*, 2017, **45**, 5350-5355.

12 H. Y. Chen, R. A. Oweini, J. Friedl, C. Y. Lee, L. L. Li, U. Kortz, U. Stimming and M. Srinivasan, *Nanoscale*, 2015, **7**, 7934-7941.

13 J. J. Zhu, R. B. Vilaua and P. G. Romero, *Electrochim. Acta*, 2020, **362**, 137007.

14 V. Ruiz, J. S. Guevara and P. G. Romero, *Electrochem. Commun.*, 2012, **24**, 35-38.

15 J. S. Guevar, V. Ruiz and P. G. Romero, *J. Mater. Chem. A*, 2014, **2**, 1014-1021.

16 C. L. Wang, S. Rong, Y. Q. Zhao, X. M. Wang and H. Y. Ma, *Transit. Metal Chem.*, 2021, **46**, 335-343.

17 J. X. Wang, L. Zhang, L. J. Zhao, T. Li and S. B. Li, *J. Mol. Struct.*, 2021, **1231**, 129966.

18 M. Yang, S. Rong, X. M. Wang, H. Y. Ma, H. J. Pang, L. C. Tan and Y. X. Jiang, *ChemNanoMat*, 2021, **7**, 299–306.

19 J. Q. Qin, F. Zhou, H. Xiao, R.Y. Ren and Z.S. Wu, *Sci. China Mater.*, 2018, **61**, 233-242.

20 J. S. Guevara, V. Ruiza, P. G. Romero, *Phys. Chem. Chem. Phys.*, 2014, **16**, 20411-20414.